Relationship between Shot Peening Surface Strain Layer and the Fatigue Strength of High-Strength Alluminium Alloy

Wang Renzhi, Li Xiangbin and Wu Hen, Institute of Aeronautical Materials, Beijing, China

Introduction

The provious investigation about the influence of shot peening (SP) on the fatigue strength of aluminium alloy (1-3) have pointed out that shot peening does not affect the fatigue strength at lower stress near the fatigue limit, although it has pronounced influence on the fatigue strength at higher stress level in S-N curves. Besides, the influence of the maximum value and the distribution of residual stress (RS) induced by SP on the fatigue behavior have been seldom investigated recently, although a lot of papers about the relation between the fatigue strength and RS have been reported. Therefore the relationship between the fatigue behavior and SP effect as well as the optimum RS field of high strength aluminium alloy have been investigated in the present article.

Materials and experiments

The rotating bending fatigue specimen (diameter 9 mm) used was high strength aluminium alloy LC9, equivalent to 7075 alloy, quenched and aged to 490 MPa tensile strength and 410 MPa yield strength. In order to investigate the effect of the deformed micro-structure, compressive RS and surface roughness on the fatigue properties, 4 kinds of specimens with different surface conditions were prepared. The depth of the surface plastically deformed microstructure and compressive RS for different specimens were listed in Table 1.

Table 1. The surface state of different specimens

No	Specimen surface state	Depth of surface plastic deformation (μm)	Surface residual stress (MPa)	Depth of compressive residual stress (μm)
A	Grinding(G)+Electro-polishing (EP)	~ 0	0	0
B	G	~ 30	-150	~ 20
C	G+Shot-peening (SP)	~ 80	-168	~ 450
D	G+SP+EP(relieved ~35 μm depth)	~ 45	-250	~ 400
E	G+SP+EP (~ 80 μm)	⩽ 10	-220	~ 370

Experimental results and discussion

After shot peening the surface cyclic strain layer is produced in which two changes occur: compressive RS and plastically deformed microstructure (4). In some cases these changes appear to be

beneficial factors for improving fatigue properties and are called as stress strengthening (SS) and microstructure strengthening (MS). In the other hand, the higher roughness resulted by shot peening can deteriorate the fatigue strength. The testing results of the influence of different factors on the fatigue strength are discripted as follows.

1. Effect of residual stresses on the fatigue strength

The distributions of RS induced with the depth are shown in Fig.1. The depth of compressive RS is about 450μm. The continuous diffraction line (222) can be obtained only using incident X-ray oscillation method (5), because LC9 is the material with a coarse grain. But it can be obtained from the surface strain layer using ordinary X-ray method. According to the diffraction line change from continuous to discontinuous and the slip band pattern in the surface strain layer, the depth of plastically deformed microstructure after SP can be determined, about 80 μm. In order to distinguish SS from MS factors, specimen E was prepared which is only single SS specimen. Specimen D exhibits both SS and MS. Specimen A is the specimen with neither SS nor MS. The rotating bending fatigue S-N curves for different kinds of specimens are shown in Fig.2.

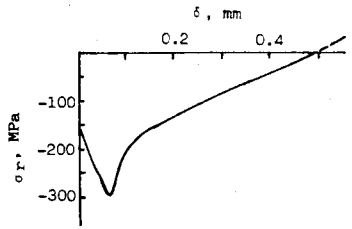

Fig. 1: Residual stress distribution in the surface layer

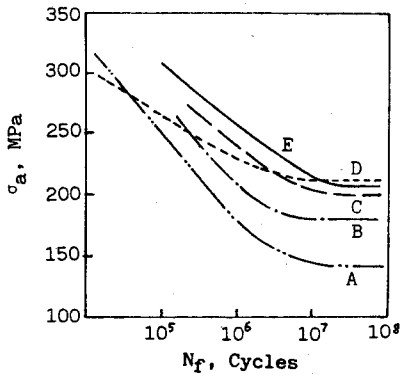

Fig. 2: Rotating bending fatigue S-N curves of 5 kinds of specimens

It is known that RS can be relaxed under the action of cyclic stresses. The stress relaxation (SR) can be divided into two classes: static load relaxation (SLR) and dynamic load relaxation (DLR). The SLR occurs in the early 1 - 5 cycles during fatigue process and for aluminium alloy it depends on both yield strength, σ_s, and cyclic compressive stress level, σ_a. The stress determination of SP specimens before and after fatigue testing is shown that the relationship between RS after relaxation, σ_r', σ_s and σ_a has following form

$$\sigma_r' = \sigma_s - \sigma_a$$

After SLR, the resulting stress distributions of specimen D with the depth, δ, are shown in Fig. 3 (specimen E has the similar stress distribution tendency with specimen D). The compressive stress in the outer surface layer decrease with the increase of σ_a, and tensile stress level at the surbsurface layer increases gradually. The fatigue crack may be only initiated at the certain subsurface positions where the tensile stress level exceeds the fatigue limit, σ_{-1}, of specimen A. Therefore, the area surrounding by $(\sigma_a+\sigma_r')-\delta$

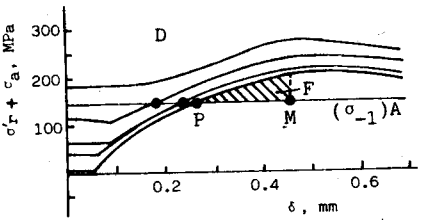

Fig. 3: $(\sigma_a+\sigma_r')-\delta$ curves of specimen D

curve and the horizontal line $(\sigma_{-1})_A$ (exactly the volume surrounding by both curved surface and plane) is the place in which the fatigue cracks have priority to initiate for the SS specimens. It can be assumed that there is the area PMN of the largest probability in which the fatigue cracks have priorty to initiate, representing as F (Fig. 3). With increasing σ_a, the value F not only increases but its place also moves to the surface. Considering the applied cyclic stress at which the fatigue cracks begin to nucleate at the specimen surface, the curves consisted of P and M points with different σ_a are shown in Fig. 4 and Fig. 5 respectively for specimens D and E.

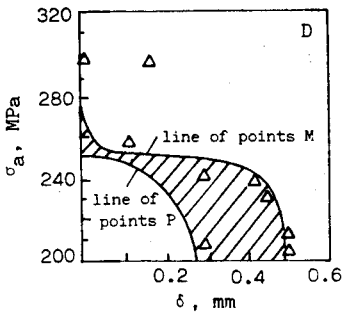

Fig. 4: Relationship between positions of points of P and M and σ_a for specimen D

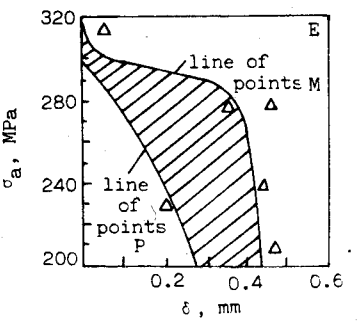

Fig. 5: Relationship between positions of points of P and M and σ_a for specimen E

The experimental points obtained from the specimen fractoraphs are shown in the same figure too. Great majority of the testing points fall in the range between the P and M curves.

Besides, the polished depth ($\sim$ 35 μm) of specimen D is thinner than that of specimen E. After eletropolishing many pits with 0.1 mm diameter and 0.01 mm depth remain at the surface of specimen D, whereas specimen E exhibits a smooth surface. Specimen D appears to be higher RS relaxation than that of specimen E due to the stress concentration effect at the root of the pit. Therefore, the stress level of specimen D at which the fatigue cracks begin to initiate at the surface is lower than that of specimen E: σ_a = 250 MPa for D and σ_a = 300 MPa for E (see Fig. 4 and Fig. 5)

2. Effect of deformed microstructure on the fatigue strength

The electron microscopic observations point out that the cell structure appers in the surface strain layer having a higher dislocation density. The dislocation motion from the subsurface to the surface under cyclic stresses action can be effectively prevented by the surface strain layer. The metallographic observations of the slip band at the surface during the fatigue process are shown that for specimen A the coase inhomogeneous slip bands occur the space of which is about 2.37 μm under σ_a=200 MPa, N=3x10^4 (Fig. 6a), whereas it does not appear under the same condition for peened specimen (electropolished depth 15 μm after SP). Increasing the cyclic stress to 250 MPa, the slip bands with 1.48 μm space occur after N=5.8x10^6 cycles for peened specimen and distribute homogeneously at the surface (Fig. 6b).

The deformed microstructure and RS can be also introduced by grinding. It can be seen from Table 1 that the grinded specimen B exhibits a

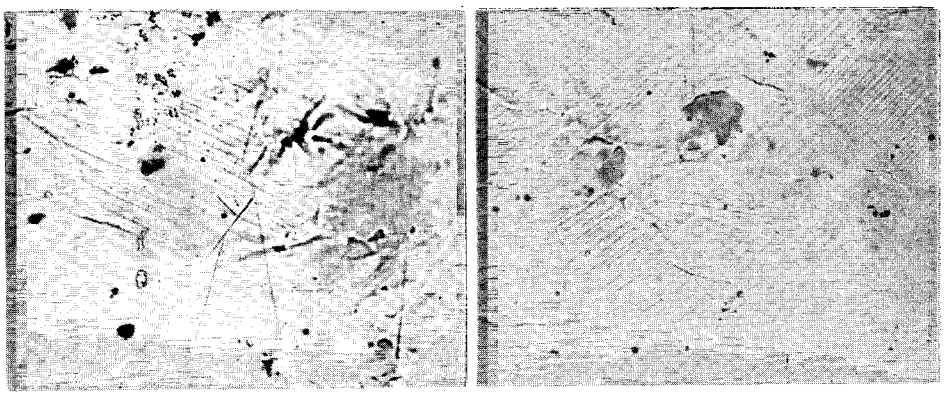

(a) (b)

Fig. 6: Slip band feature formed in the fatigue process: (a) specimen A; (b) specimen D, 500X

small depth of RS (~20 μm) and the similar depth of deformed microstructure, equivalnt to specimen D. Therefore specimen B can be regarded as a single MS specimen. The role of the single MS for improving fatigue behavior can be obtained from the comparisions of S-N curves between specimens A and B (See Fig. 2).

3. Effect of the surface roughness on the fatigue strength

Comparing the S-N curves of specimens C, D and E (Fig. 2), the order of fatigue limit ($N=2\times10^7$) is $(\sigma_{-1})_D \simeq (\sigma_{-1})_E > (\sigma_{-1})_C$. The RS relaxation due to higher stress concentration at the root of pits causes the shift of F area from inner to the surface. At the higher stress range of S-N curves, however, specimen C exhibits much higher fatigue strength than that of A, B and D due to the steaty effect of deformed microstructure although RS relaxation has taken place seriously during fatigue testing. Specimen E with lower roughness has higher fatigue strength than that of specimen C in the higher stress range of S-N curve.

4. Quantitative evaluation of the contributions of the MS, SS and surface roughness

Comparing the S-N curves shown in Fig. 2, the contributions of different factors to the fatigue limit ($N=2\times10^7$) can be summarized as follows:

1) Microstructure strengthening contribution:

$$(\Delta\sigma_{-1})_{MS} = (\sigma_{-1})_B - (\sigma_{-1})_A = 180-140 = 40 \text{ MPa}$$

2) Stress strengthening contribution:

$$(\Delta\sigma_{-1})_{SS} = (\sigma_{-1})_E - (\sigma_{-1})_A = 210-140 = 70 \text{ MPa}$$

3) Synthetic contribution of MS and SS:

$$(\Delta\sigma_{-1})_{MS} + (\Delta\sigma_{-1})_{SS} = 40+70 = 110 \text{ MPa}$$

4) The loss of fatigue limit due to the surface roughness:

$$[(\sigma_{-1})_A+(\Delta\sigma_{-1})_{MS}+(\Delta\sigma_{-1})_{SS}] - (\sigma_{-1})_C = 250-200 = 50 \text{ MPa}$$

It can be concluded that the largest contribution is the SS and then the MS, and the higher surface roughness the lower fatigue limit of materials.

5. The optimum residual stress field

The SLR and DLR of specimen D are shown in Fig. 7. It can be deduced that at high σ_a range $(\Delta\sigma_r/\sigma_r)_{static} > (\Delta\sigma_r/\sigma_r)_{dynamic}$, whereas near the fatigue limit $(\Delta\sigma_r/\sigma_r)_{static} < (\Delta\sigma_r/\sigma_r)_{dynamic}$.
In order to avoid the SLR of aluminium alloy used the maximum value of compressive RS should be close to the optimum RS, which is

$$(\sigma_r)_{op} = \sigma_s - \sigma_{-1} = 410-210 = 200 \text{ MPa}$$

In fact, it is difficult to obtain the optimum RS by means of SP. However RS can be relaxed to the expected optimum RS value by means of following heat treatment after SP (See Fig.8). This stress relaxation due to the thermal activation can not cause pronounced fatigue damage in the material. The fatigue test results of high strength steel have proved the conclusion mentioned above (6).

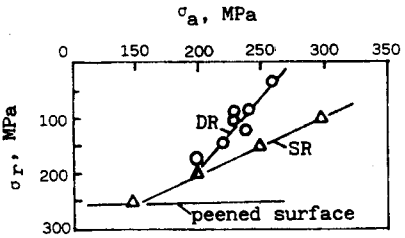

Fig. 7: Static and dynamic relaxation under different σ_a of specimen D

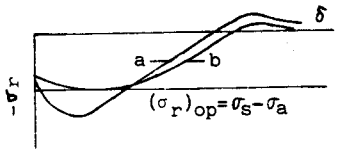

Fig. 8: Schematic diagram of RS distribution: a-σ_r-δ curve after SP; b-σ_r-δ curve of heat-treated specimen after SP

Summary

From the data presented in this article some conclusions can be deduced, refering to the material, specimen and load conditions used here.

1) For high strength aluminium alloy, shot peening can not only improve the fatigue strength at higher range of S-N curve but also increase the fatigue properties near the fatigue limit.

2) Stress and microstructure strengthening are two strengthening factor improving the fatigue strength of materials, whereas the poor roughness is the unfavarable factor for the fatigue behavior of materials.

3) There exists an optimum residual stress field induced by shot peening for the high strength aluminium alloy.

References

(1) J.E. Campbell, Metal and Ceramics Information Center, 1971
(2) G.S. Was, R.M. Pelloux and M.C. Frabolot, Proceedings of ICSP-1, Paris, September (1981) 445.
(3) A. Snowman and R.G. Schmidt, Proceedings of ICSP-1, Paris, September (1981) 13.
(4) Wang Renzhi, Li Xiangbin, Tan Yonggui and Yan Minggao, Proceedings of ICSP-1, Paris, September (1981) 185.
(5) Wang Renzhi, Acta Metallurgica Sinica 18 (1982) 493 (in Chinese)
(6) Qiu Qiong, Wang Renzhi, Proceedings of ICSP-3, Garmisch-Partenkirchen (FRG), October 12-16, (1987).